Transportable energy storage for more resilient distribution systems with multiple microgrids

Yao, Shuhan; Wang, Peng; Zhao, Tianyang

2019

Yao, S., Wang, P., & Zhao, T. (2019). Transportable energy storage for more resilient distribution systems with multiple microgrids. IEEE Transactions on Smart Grid, 10(3), 3331-3341. doi:10.1109/TSG.2018.2824820

https://hdl.handle.net/10356/89545

https://doi.org/10.1109/TSG.2018.2824820

Transportable Energy Storage for More Resilient Distribution Systems With Multiple Microgrids

Shuhan Yao, *Student Member, IEEE*, Peng Wang, *Fellow, IEEE*, and Tianyang Zhao, *Member, IEEE*

***Abstract*—Transportable energy storage systems (TESSs) have great potential to enhance resilience of distribution systems (DSs) against large area blackouts. A joint post-disaster restoration scheme for TESS and generation scheduling in microgrids (MGs) and network reconfigurations is proposed to minimize the total system cost, including customer interruption cost, generation cost, and TESS related costs. A temporal–spatial TESS model which is related to both transportation networks and DSs is proposed to represent the difference between TESS and ESS in terms of flexibility and cost reduction of ESS sharing among MGs. The proposed restoration problem is formulated as a mixed-integer linear programming with considering various network and TESS constraints. The proposed model and scheme are tested in a modified 33-bus test system with three MGs and four TESSs. The results verify that a distribution system with TESS is more resilient compared with conventional ESS because of the benefit from total cost reduction.**

***Index Terms*—Transportable energy storage systems, microgrids, service restoration, resilience, time-space network.**

NOMENCLATURE

Acronyms

DS	Distribution system
MG	Microgrid
TESS	Transportable energy storage system
DG	Distributed generator
DER	Distributed energy resource
TSN	Time-space network
MILP	Mixed-integer linear programming
VSP	Vehicle scheduling problem
SOC	State of charge.

Manuscript received November 20, 2017; revised February 27, 2018; accepted April 5, 2018. Date of publication April 9, 2018; date of current version April 19, 2019. This work was supported by Future Resilient Systems, Singapore-ETH Centre through the National Research Foundation of Singapore under Its Campus for Research Excellence and Technological Enterprise program. Paper no. TSG-01698-2017. *(Corresponding author: Tianyang Zhao.)*

S. Yao is with the Institute of Catastrophe Risk Management, Interdisciplinary Graduate School, Nanyang Technological University, Singapore 639798 (e-mail: syao002@e.ntu.edu.sg).

P. Wang is with the School of Electrical and Electronic Engineering, Nanyang Technological University, Singapore 639798 (e-mail: epwang@ntu.edu.sg).

T. Zhao is with Energy Research Institute at NTU, Nanyang Technological University, Singapore 639798 (e-mail: zhaoty@ntu.edu.sg).

Color versions of one or more of the figures in this paper are available online at http://ieeexplore.ieee.org.

Digital Object Identifier 10.1109/TSG.2018.2824820

Indices and Sets

$\mathbf{N}$	Set of DS buses, indexed by i, j, k
$\mathbf{E}$	Set of DS branches, indexed by (i, j)
$\mathbf{T}$	Set of time spans, indexed by t, $T = \lvert\mathbf{T}\rvert$
$\mathbf{\Psi}(i)$	Set of buses connected to bus i by a branch
$\mathbf{M}$	Set of MGs, indexed by m, u
$\mathbf{M}_{\mathrm{v}}$	Set of virtual nodes in TSN
$\mathbf{\Omega}$	Set of TESSs, indexed by ω
$\mathbf{Z}$	Set of arcs in TSN, indexed by (m, u)
$\mathbf{Z}_m^+$	Set of arcs in TSN starting from MG m
$\mathbf{Z}_m^-$	Set of arcs in TSN ending at MG m.

Parameters

ΔT	Time span
r_{ij}, x_{ij}	Resistance and reactance of line (i, j)
φ_i	Power factor of load at bus i
PD_i^t, QD_i^t	Active/reactive load at bus i in time span t
$S_{ij}^{\max}$	Apparent power capacity of line (i, j)
$V_i^{\max}$, $V_i^{\min}$	Maximum/minimum voltage magnitude at bus i
$P_{\mathrm{DG},m}^{\max}$, $Q_{\mathrm{DG},m}^{\max}$	Maximum active/reactive power of equivalent dispatchable DG in MG m
$E_{\mathrm{DG},m}^{\max}$, $E_{\mathrm{DG},m}^{\min}$	Energy capacity/minimum reserve in MG m
$P_{\mathrm{D},m}^t$, $Q_{\mathrm{D},m}^t$	Local active/reactive load in MG m in time span t
η_{ch}, η_{dch}	Charging/discharging efficiency of TESSs
$P_{\mathrm{ch}}^{\max}$, $P_{\mathrm{dch}}^{\max}$	Maximum charging/discharging power of TESSs
$SOC_{\max / \min}$	Maximum/Minimum SOC level of TESSs
$E_{\mathrm{TESS}}^{\mathrm{cap}}$	Energy capacity of TESSs
W_i	Unit interruption cost for load at bus i
$C_{\mathrm{gen},m}$	Unit generation cost for the DGs in MG m
$C_{\mathrm{tran},\omega}$	Unit transportation cost for the TESS ω
$C_{\mathrm{bat},\omega}$	Unit battery maintenance cost for the TESS ω.

Variables

PG_i^t, QG_i^t	Active/reactive power generated at bus i in time span t
$PD_{r,i}^t$, $QD_{r,i}^t$	Load restored at bus i in time span t
P_{ij}^t, Q_{ij}^t	Active/reactive power from bus i to bus j in time span t
V_i^t	Voltage magnitude at bus i in time span t
α_{ij}	Binary variable, 1 if the line (i, j) is connected, 0 otherwise

β_{ij}	Binary variable, 1 if bus j is the parent of bus i, 0 otherwise
$P^t_{\mathrm{DG},m}$, $Q^t_{\mathrm{DG},m}$	Active/reactive power generated of equivalent dispatchable DG in MG m in time span t
$E^t_{\mathrm{DG},m}$	Energy of equivalent dispatchable DG in MG m by the end of time span t
$I^t_{\mathrm{ch},\omega}$, $I^t_{\mathrm{dch},\omega}$	Binary variables, charging/discharging state of TESS ω in time span t
$\zeta^t_{\omega,mu}$	Binary variables, 1 if TESS ω is on arc (m, u) in time span t, 0 otherwise
$P^t_{\mathrm{ch},\omega m}$, $P^t_{\mathrm{dch},\omega m}$	Charging/discharging power of TESS ω from/to MG m in time span t
SOC^t_ω	SOC of TESS ω by the end of time span t.

I. Introduction

Large area blackouts lead to widespread catastrophic consequences for economy and society [1], [2]. It highlights the importance of power systems resilience against major disruptions [3], [4], especially for DSs [5]–[7]. In a more resilient DS, electric service restoration can be implemented efficiently using stationary [8], [9] and transportable sources [10], [11]. After a disaster, stationary sources, e.g., DERs and MGs, can be adopted for one island of the DS [8], [9]. Equipped with vehicles, transportable sources, e.g., TESSs, have great potential to enhance the resilience through optimal scheduling among multiple islands within the DS.

Considerable progress has been made with respect to the utilization of stationary sources in DS restoration [12], [13]. DGs are widely adopted in the restoration when the DS is isolated from the main grid [14]. When DGs are insufficient to meet the energy requirements, MGs can be used to aggregate a wide range of DERs for service restoration [15]–[17]. In addition, the DS can be sectionalized into multiple islands, where each island has one MG [18]. These researches illustrate that DS can benefit enormously from the stationary DERs, especially MGs, in enhancing resilience against large area blackouts. Furthermore, with the increasing penetration of public charging/discharging facilities [19], [20], MGs provide opportunities to integrate TESSs for DS service restoration.

For the integration of TESSs, some researches have been conducted to apply TESSs into power systems operation under both normal [21], [22] and extreme conditions [23]. Under normal conditions, TESSs are utilized to provide ancillary services to both transmission networks [24], [25] and DSs [26]. For transmission networks, TESSs are applied to realize load shifting in [21] and [22]. To alleviate the transmission line congestion and reduce the operating cost, a battery-based energy transportation system integrated unit commitment problem is presented in [24]. Aside from boosting system economics, the battery-based energy transportation system is used to reduce the wind power curtailment in [25]. To regulate the voltage profiles in DSs, a transition model is developed to schedule mobile energy storage systems' position and operation plans in [26].

Under extreme conditions, TESSs can be scheduled in pre and post stage of the extreme events. Before the advent of extreme events, TESSs have been deployed as uninterruptible power supplies in [27]. In [10], electric buses and transportable batteries are allocated as proactive preparedness for hurricanes. A joint pre and post-dispatch framework is proposed for the mobile emergency generators, where the position is optimized before natural disasters and real-time output is optimized after the disasters in [11]. As there is no trip chain scheduling, one mobile emergency generator is dispatched to form MGs and then stand still at the same place to serve as the root bus [11]. In conclusion, the status of TESSs scheduling for resilient response to blackouts is ether pre-positioned or only implemented one time after outages, which is not coordinated with the network reconfiguration and operation of DSs.

The scheduling of TESSs and network reconfiguration of DSs should be jointly optimized in the post-disaster restoration. After a disaster, there exist multiple faults in the DS, and the network reconfiguration is necessary to improve the resilience via forming multiple islands [16], [17]. TESSs can affect the power balance in each island through a sequence of trips, e.g., an optimal scheduling of TESSs [24]. To the best of our knowledge, a joint scheduling of TESSs and network reconfiguration in the post-disaster restoration has not been considered yet, especially from the resilience perspective.

In this context, this paper aims to fulfill the gap in the application of TESSs into DS restoration. A joint post-disaster restoration scheme is proposed, in which TESSs are dynamically scheduled in coordination with DS reconfiguration through MGs, to minimize the total cost in the wake of catastrophes. Specifically, MGs make the most of available generating resources and act as root buses to dynamically form islands for loads pickup, while the TSN is adopted and customized in VSP [28], [29] to mathematically model the scheduling problem of TESSs. The optimization problem is formulated as a MILP model. Main contributions are concluded as follows.

1) A joint post-disaster restoration scheme for coordination of TESSs and DSs with multiple MGs is proposed to bridge the gap in the application of TESSs to achieve a more resilient DS. A temporal-spatial TESS model, connecting the transportation networks and DSs, is proposed to represent the difference between TESS and ESS in terms of flexibility and cost reduction of ESS sharing among MGs.

2) The total cost, considering both the benefits (mitigating the customer interruption cost) and operation costs (MG generation cost, and TESS transportation cost and battery maintenance cost), is proposed to evaluate the feasibility of using TESS in DS restoration.

The remainder of the paper consists of five sections. Section II defines the resilience and illustrates the system architecture in detail. Section III presents the modeling of TESSs. Section IV proposes the mathematical formulation of a joint post-disaster restoration scheme. Section V provides the numerical results and analysis, and the paper is summarized in Section VI.

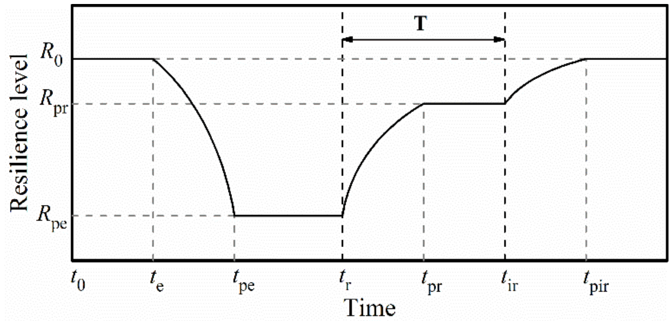

Fig. 1. A conceptual resilience curve associated with an event.

II. Resilient Distribution Systems With Transportable Energy Storage Systems

This section gives an introduction to power system resilience evaluation and TESSs. Due to the advantage of transportability, TESSs are utilized to assist DS restoration. A novel application of TESS in DS is illustrated to propose a joint post-disaster restoration scheme.

A. Power System Resilience Evaluation

Resilience is defined as the ability to prepare for and adapt to changing conditions and withstand and recover rapidly from disruptions [6]. A conceptual resilience curve associated with an event in [30] is adopted in this work for illustration, as shown in Fig. 1. R refers to an index of system resilience level. The system states involve: pre-disturbance resilient state (t_0, t_e), event progress (t_e, t_{pe}), post-event degraded state (t_{pe}, t_r), restorative state (t_r, t_{pr}), post-restoration state (t_{pr}, t_{ir}) and infrastructure recovery (t_{ir}, t_{pir}). Specifically, a catastrophic event strikes the DS at t_e, resulting in a prolonged outage as electric service to end users is disrupted. The faults and consequences are identified in (t_{pe}, t_r) to improve DS operator's situational awareness. The proposed joint restoration scheme is implemented from t_r to enhance system resilience level to R_{pr}. The DSs remains in the post-restoration state until the upstream transmission systems come back into operation.

In this paper, the concerned period is (t_r, t_{ir}), i.e., the restorative state and post-restoration state. In the aftermath of extreme events, by analyzing the outage information, the distribution system operator is able to estimate the time period for full recovery [10], [18]. It is assumed that the upstream transmission system is restored at t_{ir} and the joint restoration scheme for DS is carried out over the optimization horizon $\mathbf{T}$, as shown in Fig. 1.

In the wake of major disturbances, a restoration scheme is implemented over the optimization horizon $\mathbf{T}$ to reach a higher level of R_{pr}. The resilience level, R_{pr}, is the index to quantify the performance of a distribution system.

B. Transportable Energy Storage Systems

TESSs are truck-mounted energy storage systems characterized by utility-scale capacity [23]. In a TESS, an array of batteries is installed on a transport truck, where power converters and controllers are integrated. Under the demonstration stage, TESSs are attractive players in the resilient power systems, along with the cost reduction and profitable benefits.

Various demonstration projects of TESS application have been deployed in recent years. In the U.S., electric utility company Premium Power's 0.5-MW/2.8-MWh transportable Zinc-Bromine energy storage system was deployed by Electric Power Research Institute (EPRI) [31]. EPRI and Department of Defense of the U.S. initiated a project to demonstrate a containerized grid support storage system featuring utility capacity up to 2 MWh committed to enhancing energy security at military facilities [32]. Li-ion developer Altair Nanotechlogoies has 1-MW/250-kWh trailer-mounted Li-ion battery systems in service with both AES corporation and PJM interconnection [31].

In comparison to stationary ESSs, TESSs have a sort of advantages in terms of transportability, operational flexibility, which enable TESS to provide power supply to critical loads under emergency conditions. Furthermore, the installed capital cost of TESS is expected to reduce to a competitive level in about 5 to 10 years [32]. TESSs have the potential to rival distributed generation units like fuel cells and micro turbines in the coming years [32].

In terms of techno-economic benefits, it is promising to utilize TESSs to provide of various ancillary services [24], [26]. For the more resilient DSs, TESSs can follow the trip chains among multiple islands to engage in the restoration. The trip chains can specify the TESSs' assigned locations in corresponding time span to describe the spatiotemporal driving pattern of TESSs.

C. Distribution System Restoration With Transportable Energy Storage Systems

A novel application of TESS in DS is studied to propose a joint post-disaster restoration scheme, which leverages TESSs and generating resources in MGs for post-disaster restoration, as shown in Fig. 2. In the aftermath of extreme events, the DS can no longer be supplied by transmission grids as a result of multiple faults across the power systems, including substation faults, broken feeders. Under this circumstance, MGs will be utilized to pick up critical loads by sectionalizing the DS into multiple islands. TESSs are assumed to be owned and controlled by utility companies, and they can be dispatched in time horizon $\mathbf{T}$. In addition, it is assumed that there exists a transportation network connecting all MGs within the DS.

The idea is to optimally coordinate scheduling of TESSs and distribution network reconfiguration with MGs, enabling a resilient service restoration in DS after natural hazards. On the one hand, the DS is reconfigured and sectionalized into a few islands through controlling the ON/OFF status of remote-controlled switches. In each island, a MG is the root bus to supply electricity to critical loads and works as an interface to couple DSs and transportation systems. On the other hand, by solving VSP, TESSs can be scheduled to travel among MGs through the transportation network to transfer energy, alleviating distribution network energy imbalance

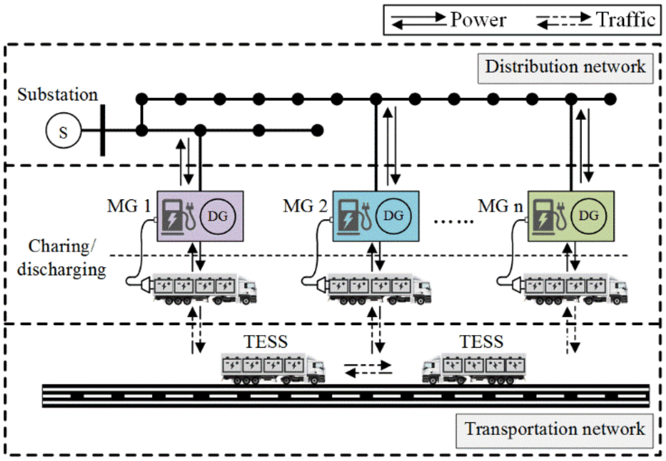

Fig. 2. Overview of system architecture.

posed by operation and topology constraints in scenarios of multiple faults, in order to improve the resilience level.

To indicate the resilience level for a DS with TESSs as shown in Fig. 2, the total cost, considering both the benefits (mitigating the customer interruption cost) and operation costs (MG generation cost, and TESS transportation cost and battery maintenance cost), is utilized. The effort is characterized by mitigating the customer interruption cost and MG generation cost. Moreover, the operation costs of TESS are considered with the transportation cost and battery maintenance cost. In this sense, the defined total cost can be adopted to evaluate the feasibility of the joint restoration scheme, and the minimization of total cost leads to an optimal restoration scheme.

III. Modeling of Transportable Energy Storage Systems

In contrast to stationary ESSs, TESSs can transport energy to designated locations over the transportation network. In order to deal with scheduling problems more efficiently in both time and spatial domains, a TSN model is adopted to model the trip chain of TESSs. This section proposes a temporal-spatial TESS model to investigate the driving dynamics and charging/discharging behaviors of TESSs, and studies their impacts on DS restoration.

A. Temporal-Spatial Constraints of Transportable Energy Storage Systems

In order to deal with scheduling problems more efficiently in both time and spatial domains, new modeling methods have been applied, such as continuous time modeling and TSN modeling [33]. In contrast to the continuous time modeling method [33], the TSN model is more suitable for scheduling problem involving both space decisions and discrete time intervals [28], which is in line with the discrete time spans in planning horizon for DS. In addition, the TSN-based scheduling model can be formulated as a MILP problem, which could be effectively solved by off-the-shelf solvers.

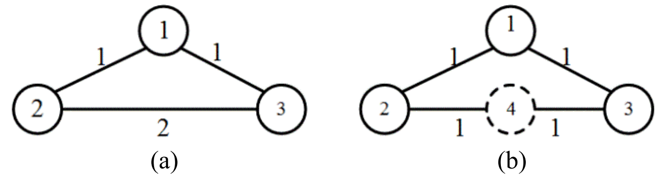

Fig. 3. Transportation network with virtual nodes.

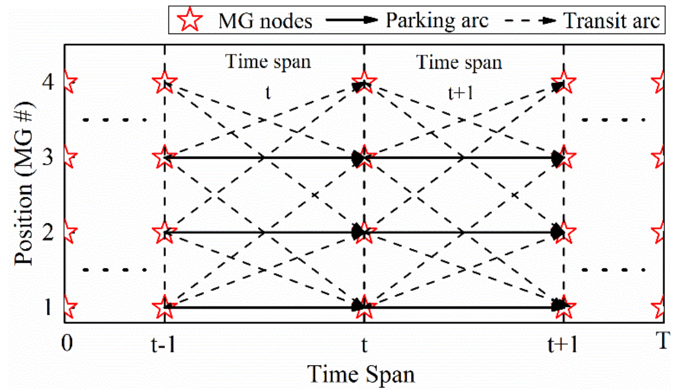

Fig. 4. Time-space network model.

A transportation network connecting multiple MGs is considered, as shown in Fig. 3. Each arc is marked with an associated travel time. For example, it takes two time spans for TESSs to travel between MG2 and MG3, whereas only one time span for any other transit. In order to enable arcs to represent the corresponding status in each time span, a virtual node, i.e., MG4 is introduced in between MG2 and MG3, so that travel time of each arc in the network is exactly one time span [24].

The transportation network with travel time is modeled by a TSN, as shown in Fig. 4, which has been broadly used to model airline and public transportation scheduling problems [28], [34]. In this work, a mathematical model for TESS scheduling problem is presented based on the TSN involving MG nodes and trip arcs. The trip chain can be represented by a sequence of arcs, which indicate the departure MG nodes and destination MG nodes in a given timetable.

As illustrated in Fig. 4, the TESSs traveling and parking behavior is described by different types of arcs to indicate the spatiotemporal dynamics of TESSs. The TSN comprises MG nodes and the arcs linking various MGs, indicating the feasible transit routes. There are two types of arcs in the TSN. One type is referred to as the transit arc, which allows TESSs to transport energy among MGs. Another type is the parking arc, which represents the TESS stays at a certain MG for exchanging power with DSs through charging or discharging. Therefore, a trip chain for each TESS can be determined to schedule TESSs to different MGs over the time horizon $\mathbf{T}$.

The TSN-based TESS model is formulated as follows.

$$\sum_{(m,u)\in \mathbf{Z}} \zeta^{t}_{\omega,mu} = 1, \forall \omega \in \mathbf{\Omega},\ t \in \mathbf{T} \tag{1}$$

$$\sum_{(m,u)\in\mathbf{Z}_m^-} \zeta_{\omega,mu}^t = \sum_{(m,u)\in\mathbf{Z}_m^+} \zeta_{\omega,mu}^{t+1}, \forall\omega\in\mathbf{\Omega},\ m\in\mathbf{M}\cup\mathbf{M}_v, t\in\mathbf{T}\backslash\{T\} \tag{2}$$

$$\sum_{(m,u)\in\mathbf{Z}_m^+} \zeta_{\boldsymbol{\omega},mu}^1 = \zeta_{\omega,m}^0, \forall\omega\in\mathbf{\Omega},\ m\in\mathbf{M}\cup\mathbf{M}_\text{v} \tag{3}$$

$$\zeta_{\omega,mu}^t + \zeta_{\omega,um}^{t+1} \le 1, \forall\omega\in\mathbf{\Omega},\ (m,u)\in\mathbf{Z}, m\ne u, t\in\mathbf{T}\backslash\{T\} \tag{4}$$

Equation (1) ensures that TESS ω can be either on transit arcs or parking arcs. Constraints (2) and (3) refer to the flow conservation for both MG nodes and virtual stations. In (2), TESS ω, which ends the trip in time span t at MG node m, is certain to keep staying on one of the arcs which start from node (t, m) in the next time span $t+1$. Particularly, constraint (3) declares the initial position. The constraint (4) guarantees that under no circumstances TESSs are able to make immediate round trip, i.e., TESSs moving from one MG to another one are not permitted to go directly back to the previous MG.

B. Operation Constraints of Transportable Energy Storage Systems

When arrives at one MG, i.e., on parking arcs shown in Fig. 4, TESS can charge from or discharge to this MG, while satisfying the following operation constraints.

$$0 \le P_{\text{ch},\omega m}^t \le \zeta_{\omega,mm}^t P_{\text{ch},\omega}^{\max}, \forall\omega\in\mathbf{\Omega},\ m\in\mathbf{M}, t\in\mathbf{T} \tag{5}$$

$$0 \le P_{\text{dch},\omega m}^t \le \zeta_{\omega,mm}^t P_{\text{dch},\omega}^{\max}, \forall\omega\in\mathbf{\Omega},\ m\in\mathbf{M}, t\in\mathbf{T} \tag{6}$$

$$0 \le \sum_{m\in\mathbf{M}} P_{\text{ch},\omega m}^t \le I_{\text{ch},\omega}^t P_{\text{ch},\omega}^{\max}, \forall\omega\in\mathbf{\Omega},\ t\in\mathbf{T} \tag{7}$$

$$0 \le \sum_{m\in\mathbf{M}} P_{\text{dch},\omega m}^t \le I_{\text{dch},\omega}^t P_{\text{dch},\omega}^{\max}, \forall\omega\in\mathbf{\Omega},\ t\in\mathbf{T} \tag{8}$$

$$I_{\text{dch},\omega}^t + I_{\text{ch},\omega}^t \le \sum_{m\in\mathbf{M}} \zeta_{\omega,mm}^t, \forall\omega\in\mathbf{\Omega},\ t\in\mathbf{T} \tag{9}$$

$$SOC_\omega^{t+1} = SOC_\omega^t - \frac{\Delta T}{E_{\text{TESS}}^{\text{cap}}}\left(\frac{\sum_{m\in\mathbf{M}} P_{\text{dch},\omega m}^{t+1}}{\eta_{\text{dch},\omega}} - \eta_{\text{ch},\omega}\sum_{m\in\mathbf{M}} P_{\text{ch},\omega m}^{t+1}\right), \quad \forall\omega\in\mathbf{\Omega},\ t\in\mathbf{T}\backslash\{T\} \tag{10}$$

$$SOC_{\min} \le SOC_\omega^t \le SOC_{\max}, \forall\omega\in\mathbf{\Omega},\ t\in\mathbf{T} \tag{11}$$

Constraints (5) and (6) establish the feasible sets of charging/discharging power of TESS ω to MG m. Equations (7) and (8) define the TESS charging/discharging constraints associated with its operation mode. The operation mode constraint is described in (9), indicating that TESS can operate in charging/discharging mode for exchanging power with MGs only if it is on parking arcs to stay in a certain MG. For instance, if TESS ω stays at any MG and we can obtain that $\sum_{m\in\mathbf{M}} \zeta_{\omega,mm}^t = 1$, thus TESS ω can be operated either in charging/discharging or idle mode, otherwise, the sign of charging/discharging status would be sandwiched to zero. Constraint (10) determines the SOC of TESS ω by the end of time span t. Finally, the SOC upper and lower bounds limitations are denoted in (11).

IV. Joint Post-Disaster Restoration Scheme

Incorporating TESSs into DSs, a more resilient restoration solution can be obtained through the coordination of TESSs and DSs. To achieve the optimal restoration, the mathematical formulation of joint post-disaster restoration scheme is presented in this section. The objective is to minimize the total cost, subject to operation and topology constraints. Partial load restoration is adopted by introducing continuous variables for each load as in [35] and [36]. Customer interruption cost is used to distinguish critical loads [37]–[39]. The objective function and constraint sets are described as follows.

A. Objective Function

The objective function aims to minimize the total cost, considering the customer interruption cost, MG generation cost, and TESS transportation cost and battery maintenance cost, as follows.

$$\min \sum_{t\in\mathbf{T}}\Bigg[\sum_{i\in\mathbf{N}} W_i\big(PD_i^t - PD_{\text{r},i}^t\big)\Delta T + \sum_{m\in\mathbf{M}} C_{\text{gen},m}P_{\text{DG},m}^t\Delta T + \sum_{\omega\in\mathbf{\Omega}} C_{\text{tran},\omega}\sum_{(m,u)\in\mathbf{Z},m\ne u}\zeta_{\omega,mu}^t + \sum_{\omega\in\mathbf{\Omega}} C_{\text{bat},\omega}\sum_{m\in\mathbf{M}}\big|P_{\text{ch},\omega m}^t + P_{\text{dch},\omega m}^t\big|\Delta T\Bigg] \tag{12}$$

The first term $\sum_{i\in\text{N}} W_i(PD_i^t - PD_{\text{r},i}^t)\Delta T$ calculates the customer interruption cost in time span t. The second term $\sum_{m\in\mathbf{M}} C_{\text{gen},m}P_{\text{DG},m}^t\Delta T$ indicates the MGs generation cost in time span t. The third term $\sum_{(m,u)\in\mathbf{Z},m\ne u} C_{\text{tran},\omega}\zeta_{\omega,mu}^t$ is regarding the transportation cost in time span t, where $\sum_{(m,u)\in\mathbf{Z},m\ne u}\zeta_{\omega,mu}^t$ describes whether the transporting cost takes effect. When it equals to 1, the TESS ω is in transit in time span t, resulting in transportation cost. Otherwise, the transportation cost would not be incurred. The last term $\sum_{\omega\in\mathbf{\Omega}} C_{\text{bat},\omega}\sum_{m\in\mathbf{M}} |P_{\text{ch},\omega m}^t + P_{\text{dch},\omega m}^t|\Delta T$ provides the TESS battery maintenance cost for charging/discharging.

B. Distribution Network Topology Constraints

The DS is modeled as an undirected graph $\mathbf{G}$=($\mathbf{N}$, $\mathbf{E}$) [16]. In the case of multiple faults, there might be some isolated areas without connection to any generating resources. These completely isolated areas will be removed. For the sake of notational simplicity, each MG m is denoted by the node i at which the MG is connected to the distribution network, i.e., $m=i$. It can be concluded that $\mathbf{M}\subseteq\mathbf{N}$.

The network reconfiguration should retain the radial structure [11], [16], [18]. There is only one MG in each island, and no loop or overlap region exists. The radiality and connectivity features in [40] are extended to the circumstance with multiple MGs over the distribution network. The formulation can be described as following.

$$\sum_{(i,j)\in\mathbf{E}} \alpha_{ij} = |\mathbf{N}| - |\mathbf{M}| \tag{13}$$

$$\beta_{ij} + \beta_{ji} = \alpha_{ij}, \forall(i,j)\in\mathbf{E} \tag{14}$$

$$\sum_{j \in \Psi(i)} \beta_{ij} = 1, \forall i \in \mathbf{N} \backslash \mathbf{M} \tag{15}$$

$$\beta_{ij} = 0, \forall i \in \mathbf{M}, j \in \Psi(i) \tag{16}$$

where $|\mathbf{N}|$ and $|\mathbf{M}|$ denote the cardinality of the set. The network reconfiguration is achieved by one-time switching operation decisions. The necessary condition for the spanning tree is denoted by (13). Equation (14) determines if a line is connected by checking that either $\beta_{ij} = 1$ or $\beta_{ji} = 1$. Equation (15) represents that every bus other than the MG buses has exactly one parent, while constraint (16) enforces that the MG buses, serving as the root buses, has no parent.

C. Operation Constraints of Distribution Systems

In this paper, a linearized DistFlow model [11], [17], [35] is adopted in the power flow analysis of DS as follows.

$$PG_i^t - PD_{\mathrm{r},i}^t = \sum_{(i,j) \in \mathbf{E}} P_{ij}^t - \sum_{(k,i) \in \mathbf{E}} P_{ki}^t, \forall i \in \mathbf{N}, t \in \mathbf{T} \tag{17}$$

$$QG_i^t - QD_{\mathrm{r},i}^t = \sum_{(i,j) \in \mathbf{E}} Q_{ij}^t - \sum_{(k,i) \in \mathbf{E}} Q_{ki}^t, \forall i \in \mathbf{N}, t \in \mathbf{T} \tag{18}$$

$$V_j^t - V_i^t \le M(1 - \alpha_{ij}) + \frac{r_{ij} P_{ij}^t + x_{ij} Q_{ij}^t}{V_0}, \forall (i,j) \in \mathbf{E}, t \in \mathbf{T} \tag{19}$$

$$V_j^t - V_i^t \ge -M(1 - \alpha_{ij}) + \frac{r_{ij} P_{ij}^t + x_{ij} Q_{ij}^t}{V_0}, \forall (i,j) \in \mathbf{E}, t \in \mathbf{T} \tag{20}$$

$$-\alpha_{ij} S_{ij}^{\max} \le P_{ij}^t \le \alpha_{ij} S_{ij}^{\max}, \forall (i,j) \in \mathbf{E}, t \in \mathbf{T} \tag{21}$$

$$-\alpha_{ij} S_{ij}^{\max} \le Q_{ij}^t \le \alpha_{ij} S_{ij}^{\max}, \forall (i,j) \in \mathbf{E}, t \in \mathbf{T} \tag{22}$$

$$-\sqrt{2} \alpha_{ij} S_{ij}^{\max} \le P_{ij}^t + Q_{ij}^t \le \sqrt{2} \alpha_{ij} S_{ij}^{\max}, \forall (i,j) \in \mathbf{E}, t \in \mathbf{T} \tag{23}$$

$$-\sqrt{2} \alpha_{ij} S_{ij}^{\max} \le P_{ij}^t - Q_{ij}^t \le \sqrt{2} \alpha_{ij} S_{ij}^{\max}, \forall (i,j) \in \mathbf{E}, t \in \mathbf{T} \tag{24}$$

$$V_i^{\min} \le V_i^t \le V_i^{\max}, \forall i \in \mathbf{N} \backslash \mathbf{M}, t \in \mathbf{T} \tag{25}$$

$$V_i^t = V_0, \forall i \in \mathbf{M}, t \in \mathbf{T} \tag{26}$$

$$0 \le PD_{\mathrm{r},i}^t \le PD_i^t, \forall i \in \mathbf{N}, t \in \mathbf{T} \tag{27}$$

$$QD_{\mathrm{r},i}^t = PD_{\mathrm{r},i}^t \tan\left(\cos^{-1} \varphi_i\right), \forall i \in \mathbf{N}, t \in \mathbf{T} \tag{28}$$

Equations (17) and (18) are constraints regarding real and reactive power balance at each bus in time span t. Equations (19) and (20) enforce constraints on line voltage drop by using the big-M method [36], [41]. Constraints (21)-(24) provide the branch capacity limitations, which is a linearized approximation as given in [42]. Constraint (25) enforces the upper and lower bounds on voltage magnitude. Constraint (26) sets the voltage of MG buses to V_0. Constraints (27) and (28) require that power factor of each load should be maintained.

D. Operation Constraints of Microgrids

MGs are entities that coordinate DERs and behaves as a single producer or load from the grids's perspective [43]. In this paper, a MG is modeled as a single bus with an equivalent dispatchable DG aggregating the whole generating resources, an equivalent local load, and charging/discharging facilities. When integrated with TESS, MGs operation constraints can be expressed as follows.

TABLE I
NUMBER OF VARIABLES

Type	Binary Variables	Continuous Variables
Variables	α_{ij}, β_{ij}, $I_{\mathrm{ch},\omega}^t$, $I_{\mathrm{dch},\omega}^t$, $\zeta_{\omega,mu}$	PG_i^t, QG_i^t, $PD_{\mathrm{r},i}^t$, $QD_{\mathrm{r},i}^t$, P_{ij}^t, Q_{ij}^t, V_i^t, $P_{\mathrm{DG},m}^t$, $Q_{\mathrm{DG},m}^t$, $E_{\mathrm{DG},m}^t$, $P_{\mathrm{ch},\omega m}^t$, $P_{\mathrm{dch},\omega m}^t$, SOC_ω^t
Number of Variables	$3\lvert\mathbf{E}\rvert+(2+\lvert\mathbf{Z}\rvert)\times\lvert\mathbf{\Omega}\rvert\times\lvert\mathbf{T}\rvert$	$(2\lvert\mathbf{E}\rvert+3\lvert\mathbf{N}\rvert+2\lvert\mathbf{M}\rvert)\times\lvert\mathbf{T}\rvert+3\lvert\mathbf{M}\rvert\times\lvert\mathbf{T}\rvert+(2\lvert\mathbf{M}\rvert+1)\times\lvert\mathbf{M}\rvert\times\lvert\mathbf{T}\rvert$

$$PG_m^t = P_{\mathrm{DG},m}^t - \sum_{\omega \in \mathbf{\Omega}} P_{\mathrm{ch},\omega m}^t + \sum_{\omega \in \mathbf{\Omega}} P_{\mathrm{dch},\omega m}^t - P_{\mathrm{D},m}^t, \forall m \in \mathbf{M}, t \in \mathbf{T} \tag{29}$$

$$QG_m^t = Q_{\mathrm{DG},m}^t - Q_{\mathrm{D},m}^t, \forall m \in \mathbf{M}, t \in \mathbf{T} \tag{30}$$

$$0 \le P_{\mathrm{DG},m}^t \le P_{\mathrm{DG},m}^{\max}, \forall m \in \mathbf{M}, t \in \mathbf{T} \tag{31}$$

$$-Q_{\mathrm{DG},m}^{\max} \le Q_{\mathrm{DG},m}^t \le Q_{\mathrm{DG},m}^{\max}, \forall m \in \mathbf{M}, t \in \mathbf{T} \tag{32}$$

$$E_{\mathrm{DG},m}^{t+1} = E_{\mathrm{DG},m}^t - P_{\mathrm{DG},m}^{t+1} \Delta T, \forall m \in \mathbf{M}, t \in \mathbf{T} \backslash \{T\} \tag{33}$$

$$E_{\mathrm{DG},m}^{\min} \le E_{\mathrm{DG},m}^t \le E_{\mathrm{DG},m}^{\max}, \forall m \in \mathbf{M}, t \in \mathbf{T} \tag{34}$$

Equations (29) and (30) stand for the active and reactive power support from MGs to distribution systems via PCC bus m, considering TESS charging from and discharging to MGs. Constraints (31) and (32) enforce the real and reactive power capacity constraints upon dispatchable DG in each MG. Equation (33) calculates the energy in each MG. The energy limitations of MGs are given in (34).

Together with the TESS models in Section IV, the joint post-disaster restoration scheme is formulated as a MILP problem, which can be solved by off-the-shelf solvers effectively, and the constraints are classified into the following 5 categories.

1) Temporal-spatial constraints of TESSs: (1)-(4);
2) Operation constraints of TESSs: (5)-(11);
3) Distribution network topology constraints: (13)-(16);
4) Operation constraints of DS: (17)-(28);
5) Operation constraints of MGs: (29)-(34).

The number of variables in the formulated problem is shown in Table I.

Since distribution systems cover merely several to tens of kilometers of power supply radius due to relatively low voltage levels, so the $|\mathbf{M}|$ and $|\mathbf{Z}|$ are within acceptable range.

V. NUMERICAL RESULTS

In this section, the case studies are performed on a modified 33-bus test system [44] to corroborate the effectiveness of proposed reconfiguration method. The optimization model is implemented using MATLAB 2016a and solved by Gurobi [45] (or other off-the-shelf solvers), on a computer with an Intel Core i7 3.4GHz CPU and 8GB RAM.

A. Test Systems

The modified 33-bus test feeder is shown in Fig. 5. The entire DS is disconnected from the utility grid, the substation and three lines (1, 2), (6, 26) and (32, 33) are at fault as a result of disastrous events. In this study, loads are classified into

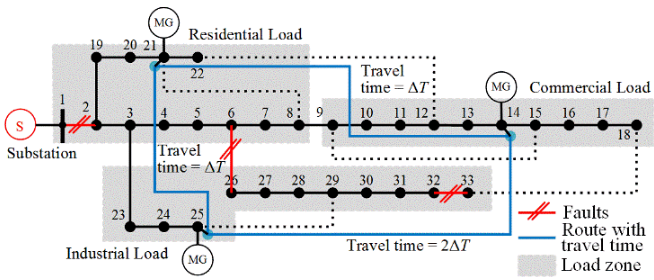

Fig. 5. A modified 33-bus test system with 3 MGs and multiple faults.

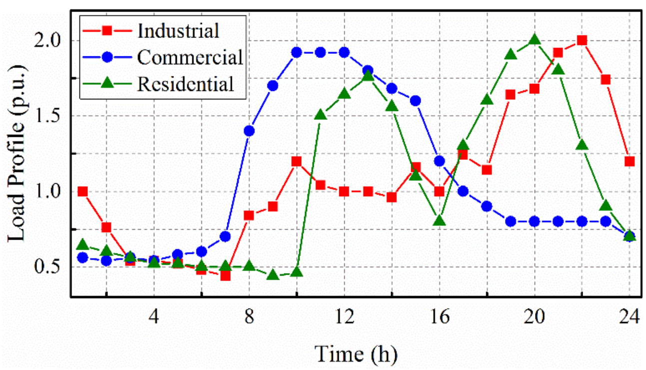

Fig. 6. Load profile.

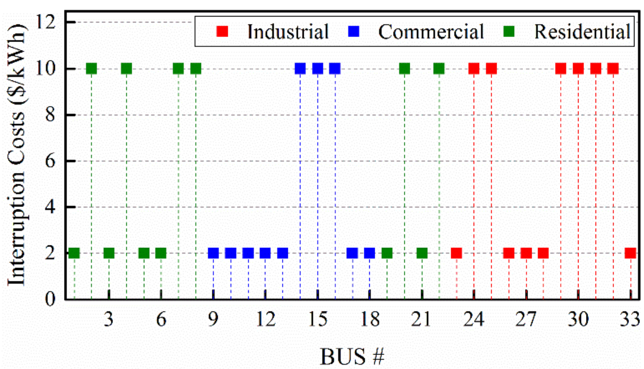

Fig. 7. Unit interruption cost.

3 types of end-use customers: industrial, commercial and residential. Fig. 6 gives the load profile [41] and Fig. 7 describes two load priority levels with unit interruption cost [37], [39].

Three MGs are connected to distribution network at buses 14, 21, 25, respectively, as depicted in Fig. 5. The transportation routes connecting three microgrids are marked with the travel time between any two microgrids. Table II provides the generation and load information for MGs. The local load in each MG follows the load profile as given in Fig. 6. Four TESSs are considered and the TESS fleet $\mathbf{\Omega}$ is supposed to be homogeneous, meaning that all TESSs have the identical properties. Parameters of TESSs are shown in Table III. The time horizon is set to 24 hours and time step is 1 hour. The unit generation cost for microgrids is \$0.5/kWh. The unit transportation cost for TESS is \$80 per transit. The unit battery maintenance cost for TESS is 0.2\$/kWh. The V_0 is set to 1.0 p.u. The $V^{\max}$ and $V^{\min}$ are 1.05 p.u. and 0.95 p.u., respectively.

TABLE II
GENERATION RESOURCES AND LOCAL LOADS FOR MICROGRIDS

MG bus #		14	21	25
Generation capacity	Real power (MW)	1.60	1.60	1.80
	Reactive power (MVar)	1.28	1.28	1.44
Energy capacity (MWh)		23.04	23.04	25.92
Minimum fuel reserve (MWh)		2.30	2.30	2.59
Local load	Peak load (MW)	0.5	0.7	0.7
	Power factor	0.9	0.9	0.9
	Load type	C	R	I

Note: I = Industrial, C = Commercial, R = Residential

TABLE III
TESS PARAMETERS

TESS #	1	2	3	4
Initial position (MG bus #)	14	21	21	25
Charging/discharging power (MW)	0.2			
Energy capacity (MWh)	1.0			
Initial SOC	0.5			
$SOC_{\max}$ /$SOC_{\min}$	0.90/0.10			
Charging/discharging Efficiency	0.95/0.95			

TABLE IV
SIMULATION STATISTICS FOR DISTRIBUTION SYSTEM RESTORATION

Results		Case 1	Case 2	Case 3
Objective (\$)	Interruption cost	115395	96639	71365
	MG generation cost	32400	32400	32400
	Transportation cost	0	0	800
	Battery maintenance cost	0	497	1875
	Total cost	147795	129536	106440
Load restoration (%)	Priority I	89.65	92.66	97.60
	Priority II	19.94	18.22	6.05
	Total	68.01	69.55	69.60

In the remaining section, three cases are investigated to show the feasibility of joint scheduling of TESSs and DSs, as follows.

Case 1) DS has microgrids without ESSs;
Case 2) DS has microgrids with stationary ESSs;
Case 3) DS has microgrids with TESSs.

B. Simulation Results

The techno-economic results under three cases are compared in Table IV.

Case 1) DS has MGs without ESSs: In this base case, MGs can utilize their available generating resources to support DS restoration. By solving the optimization problem, the network topology and optimal hourly generation dispatch for MGs are acquired. The network reconfiguration result is to open switches (3, 4), (8, 21), (12, 22), (13, 14) and (24, 25). As shown in Table IV, the total cost is \$147795, load pickup for priority I and II are 89.65% and 19.94%, respectively.

Case 2) DS has MGs with Stationary ESSs: In this case, ESSs are assumed to be fixed at MGs. In the obtained results, the open switches are (3, 4), (8, 21), (11, 12), (12, 13) and (24, 25). The total cost decreases by 12.35% to \$129536, as compared to that without ESSs in case 1. The load restored for priority I and II are 92.66% and 18.22%, respectively. It is worth noting that incorporating stationary ESSs into MGs not only reduces total cost through introducing more energy

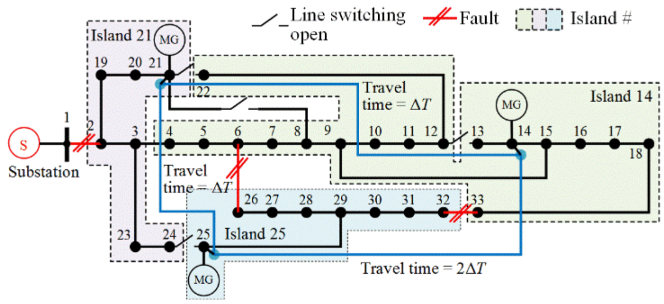

Fig. 8. Network reconfiguration result for the 33-bus test system in case 3.

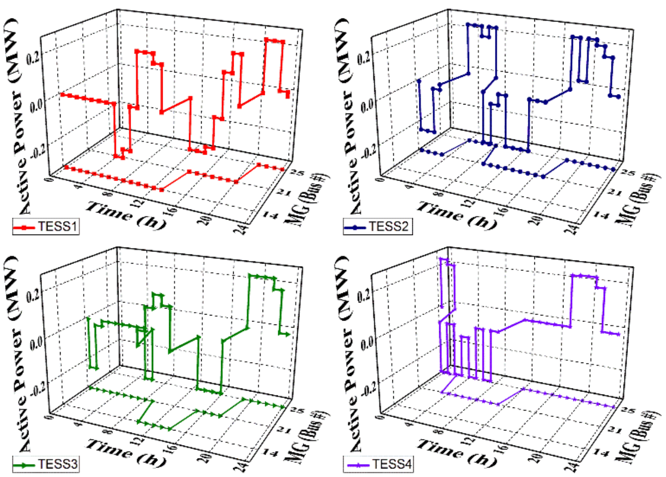

Fig. 9. TESS scheduling results in case 3.

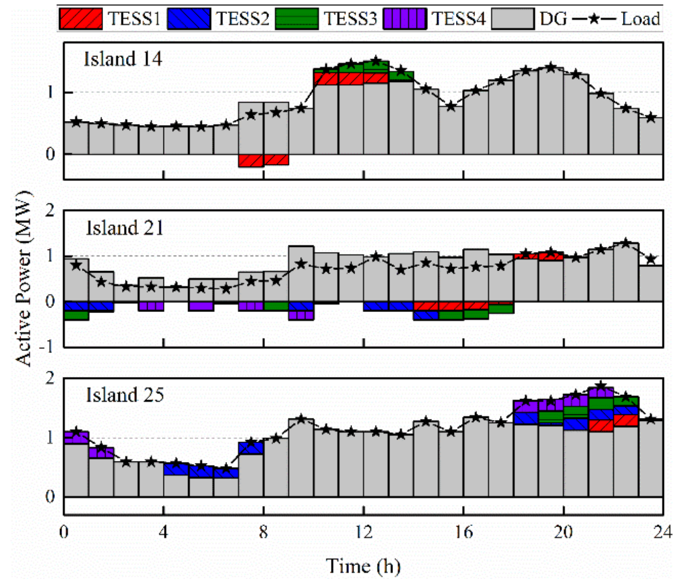

Fig. 10. Generation dispatch and load restored in case 3.

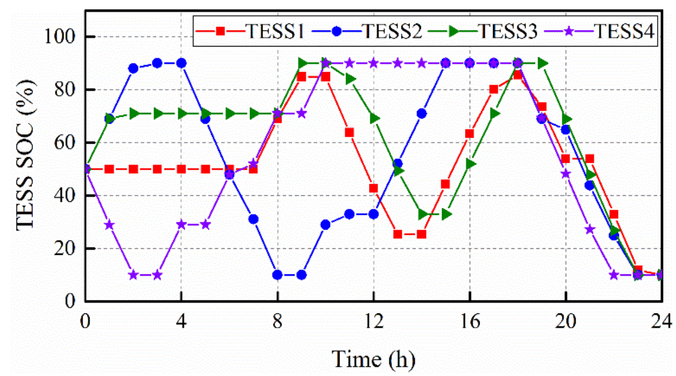

Fig. 11. SOC of TESS in case 3.

of 2 MWh, but also that stationary ESSs can work in coordination with MGs to better supply critical loads. It is noticed that total load percentage only increases by 1.54% while the load restoration for priority I rises by 3.01%. The results reveal that MGs can manage stationary ESSs to effectively restore critical loads.

Case 3) DS has MGs with TESSs: In this case, the network topology, MGs generation dispatch and scheduling of TESSs are optimized simultaneously to obtain a more resilient restoration solution. Compared with cases 1 and 2, the total cost decreases by 27.98% and 17.83%, respectively, to \$106440. The load restored for priority I enhances to 97.60% and reduces to 6.05% for priority II, respectively. These results illustrate that TESSs can improve the resilience significantly.

Fig. 8 denotes the distribution network reconfiguration results in case 3. The DS is sectionalized into 3 islands, i.e., islands 14, 21 and 25, which is denoted by the corresponding MG bus number in each island. The opening line switches are (3, 4), (8, 21), (12, 13), (21, 22), and (24, 25). In addition, each one is energized by a corresponding MG to satisfy radial topology, i.e., constraints (13)-(16).

Fig. 9 provides the charging/discharging schedule and spatiotemporal dynamics of TESSs. Note that a positive power indicates discharging of TESSs, while a negative power means the charging of TESSs. The projection on XY plane indicates the trajectory of TESSs' trip chains, while the Z-axis indicates the active power generation for each TESS. Take TESS3 for instance to illustrate the schedule. TESS3 stays at initial position MG21 for 9 hours (00:00-09:00) and charges in (00:00-02:00) and (08:00-09:00). Next, it moves from MG21 to MG14 in (09:00-10:00) and discharges for 4 hours (10:00-14:00). Then, it returns to MG21 to get charged in (15:00-18:00). The final transition is made to MG25 in (18:00-19:00) and it starts to discharge from 19:00 for 4 hours to 23:00.

Fig. 10 shows the stacked generation dispatch for MGs and TESSs. It can be seen that the active power within each island is balanced along the optimization horizon. Fig. 11 denotes the SOC of TESS and Fig. 12 depicts energy transfer from TESS to MGs through charging and discharging behaviors. Positive energy transfer represents that MG receives energy from TESSs whereas negative value represents that MG transfers energy to TESSs. It can be observed that energy transfer is mainly from MG21 to MG25 in the obtained solution.

C. Analysis and Discussions

1) Transfer of Energy Among MGs: In the simulations, it is observed that TESSs are charged where and when the power generation resource is relatively surplus for critical

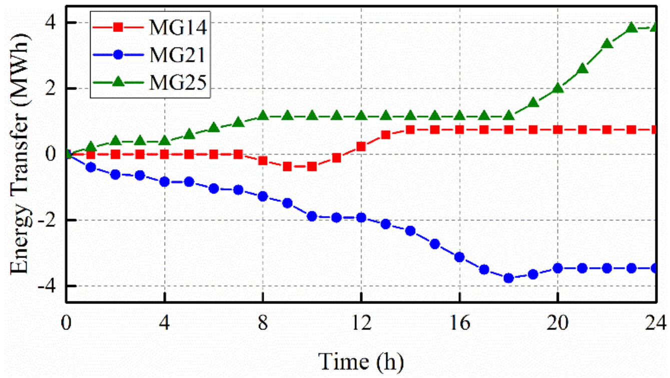

Fig. 12. Energy transfer among MGs in case 3.

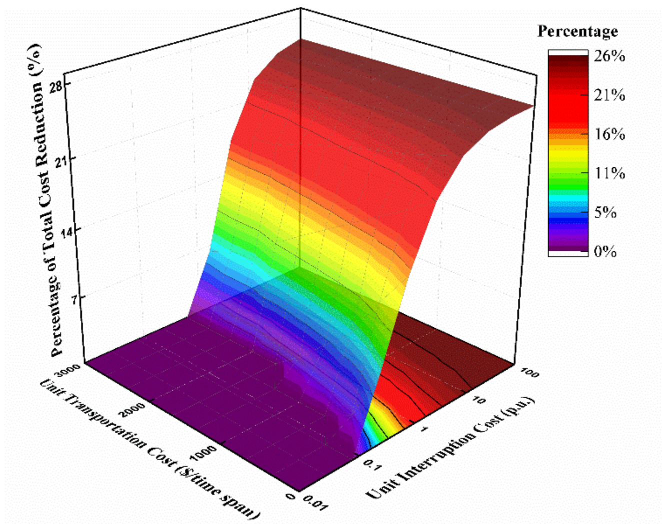

Fig. 13. Sensitivity analysis of unit interruption cost and unit transportation cost.

loads and discharged to the grid where and when the power or energy is insufficient. Energy imbalance posed by topology and operation constraints deters the effective utilization of MGs' generating resource. Thus, TESSs can decrease the total cost through transferring power and energy among MGs to serve critical loads in DS. It can be observed in Table IV that the total load restoration only rises by 0.15%, while the load restored for priority I increase by 4.97% compared to that in case 2. In this case, the TESS2 is fully charged from 00:00 to 03:00 in MG21 (see Fig. 9 and Fig. 10) to the SOC of 90% (see Fig. 11. Then TESS2 travels to MG25 in (03:00-04:00) and discharges to MG25 from 04:00 to 08:00, while the SOC reduces to the minimum level of 10%. Here, energy is transferred from MG21 to MG25 through TESS2. Similar phenomena can be observed from other TESSs.

2) Implementation of Load Shifting Within MGs: Meanwhile, TESSs can also serve as stationary ESSs to achieve load shifting within the same MGs. For instance, TESS1 stays at MG14 in (00:00-13:00), it charges in (07:00-09:00) and discharges to MG14 from 10:00 to 13:00. As noticed from Fig. 11, the SOC of TESS1 changes from 50% to 84.9% and then to 25.3%. This is because during the early time spans, the load is low as the load profile only ranges from 0.22 to 0.32, as shown in Fig. 6. TESS1 would charge in energy sufficient hours and when it comes to the peak hour, the TESS1 can discharge to MG14 to achieve efficient utilization of energy resources within MG14.

The comparison of three cases illustrates the importance of TESS transportability. The integration of TESSs would reduce the total cost through transferring energy among MGs. The application of TESSs is more effective to serve critical loads to attain effective restoration scheme, in terms of that their flexibility and transportability can tackle energy imbalance posed by topology and operation constraints. Also, the TESSs act as stationary ESSs in some time spans to perform load shifting within MGs.

3) Effect of Unit Interruption Cost and Unit Transportation Cost on Total Cost: Fig. 13 illustrates the variation of total cost reduction as a function of the unit interruption cost and unit transportation cost. The X-axis of unit interruption cost is measured in p.u. on the basis of \$10/kWh for priority I load and \$2/kWh for priority II load, which ranges from 0.01 p.u. to 100 p.u. The Y-axis of unit transportation cost is changing from \$0 to \$2000 /time span. The Z-axis of the percentage of total cost reduction is calculated by comparison between the total cost in Case 2 and Case 3.

It can be seen that the total cost reduction improves with the increasing unit interruption cost and the decreasing unit transportation cost. It is because that the lower the unit interruption cost and the higher the unit transportation cost, the fewer benefits will the DS get from the TESS and vice versa. TESS will stay at initial MGs to act as stationary ESSs if unit transportation cost is high enough (See purple area in Fig. 13). Moreover, the contours on the XY-plane further indicate the correlation between unit interruption cost and unit transportation cost given a certain level of total cost reduction.

It is also noted that the total cost reduction will remain stable as the continuous increase of unit interruption cost. The reason is that when unit interruption cost is too high and thus the transportation cost can be neglected in the scheduling of TESS, resulting in the same scheduling trip chain. In that case, the total cost is only dependent on the unit interruption cost and the total cost reduction will hit the upper bound.

Therefore, this sensitivity study can serve as a decision support tool to determine the correlation of the unit interruption cost and unit transportation cost with respect to the desired resilience level.

VI. Conclusion

The paper investigated a novel application of TESSs into DS to propose a post-disaster joint restoration scheme, which aims to minimize the total cost by scheduling TESSs in coordination with distribution network reconfiguration and MG operations. With charging/discharging facilities, MGs serve as root buses to dynamically form islands by controlling ON/OFF status of remote-controlled switches. A modified TSN-based TESS scheduling model is presented and integrated into distribution network reconfiguration to allocate TESSs among MGs. The optimization problem is formulated as a MILP model, which can derive a TESS scheduling sequence and generation dispatches for both TESSs and resources in MGs. The effectiveness of the proposed restoration scheme is demonstrated by case studies on a modified 33-bus test system.

The comparative simulations have been implemented to demonstrate the impacts of TESS on DS restoration. The TESSs transportability can efficiently transfer energy among multiple MGs within the DS in appropriate times and locations to facilitate critical loads service restoration without violating network topology and operation constraints. Meanwhile, TESSs can also serve as stationary ESSs to implement load shifting within MGs. Finally, sensitivity analysis shows impacts of unit interruption cost and unit transportation cost on the total cost, indicating the cost-effectiveness of scheduling TESS in DS restoration.

REFERENCES

[1] "Quadrennial energy review second installment: Transforming the nation's electricity system," U.S. Dept. Energy, Washington, DC, USA, Rep., 2017. [Online]. Available: https://energy.gov/policy/initiatives/quadrennial-energy-review-qer/quadrennial-energy-review-second-installment

[2] "Economic benefits of increasing electric grid resilience to weather outages," Executive Office President, Washington, DC, USA, Rep., 2013. [Online]. Available: https://energy.gov/sites/prod/files/2013/08/f2/Grid%20Resiliency%20Report_FINAL.pdf

[3] Z. Bie, Y. Lin, G. Li, and F. Li, "Battling the extreme: A study on the power system resilience," *Proc. IEEE*, vol. 105, no. 7, pp. 1253–1266, Jul. 2017.

[4] G. Huang, J. Wang, C. Chen, J. Qi, and C. Guo, "Integration of preventive and emergency responses for power grid resilience enhancement," *IEEE Trans. Power Syst.*, vol. 32, no. 6, pp. 4451–4463, Nov. 2017.

[5] C. Chen, J. Wang, and D. Ton, "Modernizing distribution system restoration to achieve grid resiliency against extreme weather events: An integrated solution," *Proc. IEEE*, vol. 105, no. 7, pp. 1267–1288, Jul. 2017.

[6] D. T. Ton and W.-T. P. Wang, "A more resilient grid: The U.S. department of energy joins with stakeholders in an R&D plan," *IEEE Power Energy Mag.*, vol. 13, no. 3, pp. 26–34, May/Jun. 2015.

[7] A. Arif, Z. Wang, J. Wang, and C. Chen, "Power distribution system outage management with co-optimization of repairs, reconfiguration, and DG dispatch," *IEEE Trans. Smart Grid*, to be published.

[8] L. Che, M. Khodayar, and M. Shahidehpour, "Only connect: Microgrids for distribution system restoration," *IEEE Power Energy Mag.*, vol. 12, no. 1, pp. 70–81, Jan./Feb. 2014.

[9] G. Jiménez-Estévez, A. Navarro-Espinosa, R. Palma-Behnke, L. Lanuzza, and N. Velázquez, "Achieving resilience at distribution level: Learning from isolated community microgrids," *IEEE Power Energy Mag.*, vol. 15, no. 3, pp. 64–73, May/Jun. 2017.

[10] H. Gao, Y. Chen, S. Mei, S. Huang, and Y. Xu, "Resilience-oriented pre-hurricane resource allocation in distribution systems considering electric buses," *Proc. IEEE*, vol. 105, no. 7, pp. 1214–1233, Jul. 2017.

[11] S. Lei, J. Wang, C. Chen, and Y. Hou, "Mobile emergency generator pre-positioning and real-time allocation for resilient response to natural disasters," *IEEE Trans. Smart Grid*, to be published.

[12] S. Chanda and A. K. Srivastava, "Defining and enabling resiliency of electric distribution systems with multiple microgrids," *IEEE Trans. Smart Grid*, vol. 7, no. 6, pp. 2859–2868, Nov. 2016.

[13] M. Panteli, D. N. Trakas, P. Mancarella, and N. D. Hatziargyriou, "Power systems resilience assessment: Hardening and smart operational enhancement strategies," *Proc. IEEE*, vol. 105, no. 7, pp. 1202–1213, Jul. 2017.

[14] Z. Wang and J. Wang, "Self-healing resilient distribution systems based on sectionalization into microgrids," *IEEE Trans. Power Syst.*, vol. 30, no. 6, pp. 3139–3149, Nov. 2015.

[15] Y. Wang, C. Chen, J. Wang, and R. Baldick, "Research on resilience of power systems under natural disasters—A review," *IEEE Trans. Power Syst.*, vol. 31, no. 2, pp. 1604–1613, Mar. 2016.

[16] Y. Xu, C.-C. Liu, K. P. Schneider, F. K. Tuffner, and D. T. Ton, "Microgrids for service restoration to critical load in a resilient distribution system," *IEEE Trans. Smart Grid*, vol. 9, no. 1, pp. 426–437, Jan. 2018.

[17] C. Chen, J. Wang, F. Qiu, and D. Zhao, "Resilient distribution system by microgrids formation after natural disasters," *IEEE Trans. Smart Grid*, vol. 7, no. 2, pp. 958–966, Mar. 2016.

[18] H. Gao, Y. Chen, Y. Xu, and C.-C. Liu, "Resilience-oriented critical load restoration using microgrids in distribution systems," *IEEE Trans. Smart Grid*, vol. 7, no. 6, pp. 2837–2848, Nov. 2016.

[19] T. Shekari, S. Golshannavaz, and F. Aminifar, "Techno-economic collaboration of PEV fleets in energy management of microgrids," *IEEE Trans. Power Syst.*, vol. 32, no. 5, pp. 3833–3841, Sep. 2017.

[20] H. S. V. S. K. Nunna, S. Battula, S. Doolla, and D. Srinivasan, "Energy management in smart distribution systems with vehicle-to-grid integrated microgrids," *IEEE Trans. Smart Grid*, to be published.

[21] M. E. Khodayar, L. Wu, and Z. Li, "Electric vehicle mobility in transmission-constrained hourly power generation scheduling," *IEEE Trans. Smart Grid*, vol. 4, no. 2, pp. 779–788, Jun. 2013.

[22] K. Knezović, S. Martinenas, P. B. Andersen, A. Zecchino, and M. Marinelli, "Enhancing the role of electric vehicles in the power grid: Field validation of multiple ancillary services," *IEEE Trans. Transport. Electrific.*, vol. 3, no. 1, pp. 201–209, Mar. 2017.

[23] B. Zhou *et al.*, "Multiobjective generation portfolio of hybrid energy generating station for mobile emergency power supplies," *IEEE Trans. Smart Grid*, to be published.

[24] Y. Sun, Z. Li, M. Shahidehpour, and B. Ai, "Battery-based energy storage transportation for enhancing power system economics and security," *IEEE Trans. Smart Grid*, vol. 6, no. 5, pp. 2395–2402, Sep. 2015.

[25] Y. Sun, J. Zhong, Z. Li, W. Tian, and M. Shahidehpour, "Stochastic scheduling of battery-based energy storage transportation system with the penetration of wind power," *IEEE Trans. Sustain. Energy*, vol. 8, no. 1, pp. 135–144, Jan. 2017.

[26] H. H. Abdeltawab and Y. A.-R. I. Mohamed, "Mobile energy storage scheduling and operation in active distribution systems," *IEEE Trans. Ind. Electron.*, vol. 64, no. 9, pp. 6828–6840, Sep. 2017.

[27] *IEEE Recommended Practice for Emergency and Standby Power Systems for Industrial and Commercial Applications*, IEEE Standard 446-1995, 1996.

[28] N. Kliewer, T. Mellouli, and L. Suhl, "A time–space network based exact optimization model for multi-depot bus scheduling," *Eur. J. Oper. Res.*, vol. 175, no. 3, pp. 1616–1627, 2006.

[29] S. Bunte and N. Kliewer, "An overview on vehicle scheduling models," *Public Transp.*, vol. 1, no. 4, pp. 299–317, 2009.

[30] M. Panteli and P. Mancarella, "The grid: Stronger, bigger, smarter? Presenting a conceptual framework of power system resilience," *IEEE Power Energy Mag.*, vol. 13, no. 3, pp. 58–66, May/Jun. 2015.

[31] "Electricity energy storage technology options," Electric Power Res. Inst., Palo Alto, CA, USA, Rep. 1020676, 2010. [Online]. Available: http://large.stanford.edu/courses/2012/ph240/doshay1/docs/EPRI.pdf

[32] "Transportable microgrid with energy storage," U.S. Dept. Defense, Arlington, VA, USA, Rep. EW-201605, 2016. [Online]. Available: https://serdp-estcp.org/Program-Areas/Energy-and-Water/Energy/Microgrids-and-Storage/EW-201605

[33] D. C. Paraskevopoulos, G. Laporte, P. P. Repoussis, and C. D. Tarantilis, "Resource constrained routing and scheduling: Review and research prospects," *Eur. J. Oper. Res.*, vol. 263, no. 3, pp. 737–754, 2017.

[34] N. Kliewer, B. Amberg, and B. Amberg, "Multiple depot vehicle and crew scheduling with time windows for scheduled trips," *Public Transp.*, vol. 3, no. 3, pp. 213–244, 2012.

[35] T. Ding, Y. Lin, G. Li, and Z. Bie, "A new model for resilient distribution systems by microgrids formation," *IEEE Trans. Power Syst.*, vol. 32, no. 5, pp. 4145–4147, Sep. 2017.

[36] T. Ding, Y. Lin, Z. Bie, and C. Chen, "A resilient microgrid formation strategy for load restoration considering master-slave distributed generators and topology reconfiguration," *Appl. Energy*, vol. 199, pp. 205–216, Aug. 2017.

[37] R. Billinton and W. Li, *Reliability Assessment of Electric Power Systems Using Monte Carlo Methods*. New York, NY, USA: Springer, 1994.

[38] "Value of customer reliability review," Aust. Energy Market Oper., Melbourne, VIC, Australia, Rep., 2014. [Online]. Available: https://www.aemo.com.au/Electricity/National-Electricity-Market-NEM/Planning-and-forecasting/Value-of-Customer-Reliability-review

[39] W. Li, *Risk Assessment of Power Systems: Models, Methods, and Applications*. Hoboken, NJ, USA: Wiley, 2014

[40] R. A. Jabr, R. Singh, and B. C. Pal, "Minimum loss network reconfiguration using mixed-integer convex programming," *IEEE Trans. Power Syst.*, vol. 27, no. 2, pp. 1106–1115, May 2012.

[41] M. R. Dorostkar-Ghamsari, M. Fotuhi-Firuzabad, M. Lehtonen, and A. Safdarian, "Value of distribution network reconfiguration in presence of renewable energy resources," *IEEE Trans. Power Syst.*, vol. 31, no. 3, pp. 1879–1888, May 2016.

[42] X. Chen, W. Wu, and B. Zhang, "Robust restoration method for active distribution networks," *IEEE Trans. Power Syst.*, vol. 31, no. 5, pp. 4005–4015, Sep. 2016.

[43] N. Hatziargyriou, H. Asano, R. Iravani, and C. Marnay, "Microgrids," *IEEE Power Energy Mag.*, vol. 5, no. 4, pp. 78–94, Jul./Aug. 2007.

[44] M. E. Baran and F. F. Wu, "Network reconfiguration in distribution systems for loss reduction and load balancing," *IEEE Trans. Power Deliv.*, vol. 4, no. 2, pp. 1401–1407, Apr. 1989.

[45] *Gurobi Optimization*. Accessed: Feb. 25, 2018. [Online]. Available: http://www.gurobi.com

Shuhan Yao (S'16) received the B.Eng. degree in electrical engineering from Chongqing University, Chongqing, China, in 2013. He is currently pursuing the Ph.D. degree with the Interdisciplinary Graduate School, Nanyang Technological University, Singapore. His research interest includes power system reliability and resilience.

Peng Wang (F'18) received the B.Sc. degree in electronic engineering from Xian Jiaotong University, Xi'an, China, in 1978, the M.Sc. degree from the Taiyuan University of Technology, Taiyuan, China, in 1987, and the M.Sc. and Ph.D. degrees in electrical engineering from the University of Saskatchewan, Saskatoon, SK, Canada, in 1995 and 1998, respectively. He is currently a Professor with the School of Electrical and Electronic Engineering, Nanyang Technological University, Singapore.

Tianyang Zhao (M'18) received the B.Sc., M.Sc., and Ph.D. degrees in automation of electric power systems from North China Electric Power University, Beijing, China, in 2011, 2013, and 2017, respectively. He is currently a Post-Doctoral Research Fellow with Energy Research Institute@Nanyang Technological University, Singapore. His research interest includes power system operation optimization and game theory.